Fate and Biological Effects of Engineered Nanomaterials

during Simulated Wastewater Treatment Processes

by

Yifei Wang

A Thesis Presented in Partial Fulfillment
of the Requirements for the Degree
Master of Science

Approved March 2012 by the
Graduate Supervisory Committee:

Paul Westerhoff, Chair
Rosa Krajmalnik-Brown
Kiril Hristovski
Bruce Rittmann

ARIZONA STATE UNIVERSITY

May 2012

ABSTRACT

As engineered nanomaterials (NMs) become used in industry and commerce their loading to sewage will increase. However, the fate of widely used NMs in wastewater treatment plants (WWTPs) remains poorly understood. In this research, sequencing batch reactors (SBRs) were operated with hydraulic (HRT) and sludge (SRT) retention times representative of full-scale biological WWTPs for several weeks. NM loadings at the higher range of expected environmental concentrations were selected. To achieve the pseudo-equilibrium state concentration of NMs in biomass, SBR experiments needed to operate for more than three times the SRT value, approximately 18 days. Under the conditions tested, NMs had negligible effects on ability of the wastewater bacteria to biodegrade organic material, as measured by chemical oxygen demand (COD). NM mass balance closure was achieved by measuring NMs in liquid effluent and waste biosolids. All NMs were well removed at the typical biomass concentration (1~2 gSS/L). However, carboxy-terminated polymer coated silver nanoparticles (fn-Ag) were removed less effectively (88% removal) than hydroxylated fullerenes (fullerols; >90% removal), nano TiO_2 (>95% removal) or aqueous fullerenes (nC_{60}; >95% removal). Although most NMs did not settle out of the feed solution without bacteria present, approximately 65% of the titanium dioxide was removed even in the absence of biomass simply due to self-aggregation and settling. Experiments conducted over 4 months with daily loadings of nC_{60} showed that nC_{60} removal from solution depends on the biomass concentration. Under conditions representative of most suspended growth biological WWTPs (e.g., activated sludge), most of the NMs

will accumulate in biosolids rather than in liquid effluent discharged to surface waters. Significant fractions of *fn*-Ag were associated with colloidal material which suggests that efficient particle separation processes (sedimentation or filtration) could further improve removal of NM from effluent. As most NMs appear to accumulate in biosolids, future research should examine the fate of NMs during disposal of WWTP biosolids, which may occur through composting or anaerobic digestion and/or land application, incineration, or landfill disposal.

ACKNOWLEDGEMENT

TABLE OF CONTENTS

LIST OF TABLES

LIST OF FIGURES

Chapter 1

INTRODUCTION

Engineered nanomaterials (ENMs) are operationally defined as materials in size between 1 to 100 nanometers with at least one dimension, where unique properties enable novel applications [1]. These novel properties that emerge at the nano-scale enable the development of materials with unique physical, chemical, and biological properties that their macromolecular counterparts do not share [1]. Today the use of nanomaterials (NMs) in commercial products is rapidly increasing. In 2006, more than 300 commercial products on the market claimed to have enhanced properties due to incorporated NMs; this number had more than quadrupled by 2010 [2, 3]. Silver is the most common NM used in products, followed by carbon-based NMs and TiO_2 [3]. A market research firm (Bins & Associates) estimates that the production of nanoparticles will be on the order of millions of tons by 2010 [4]. As a result of this increasing production and utilization, research has begun to assess the potential risks related to the presence of these ultra-small materials in the environment, including effects on bacteria, algae, fish, and other organisms [2, 5-15]. Risk assessment and management rely upon both effects data (e.g., toxicity) and exposure information. Therefore, both to assess the risk of engineered NMs in the environment and to control their release, an understanding of the processes that affect NM flux through society is critical. This has been the focus of recent exposure modeling assessments [16-21].

Of particular interest is the removal and distribution of ENMs within conventional wastewater treatment plants (WWTPs) that could be the pathways of

ENMs entering the aquatic and territory environment. Treated effluents and biosolids from WWTPs and biosolids facilities are sources for pollutants entering the environment. Many NMs used in commercial products will enter municipal or industrial wastewaters, which are collected and treated at centralized wastewater treatment plants (WWTPs) [21-23]. Although NMs may undergo transformation (e.g., dissolution of metal ions from metal-based NMs), the primary process of NM removal from sewage will be the association with biosolids, a process termed biosorption, and their subsequent removal by sedimentation and/or filtration [23-26]. Field study has discovered silver sulfide nanoparticles generated during the wastewater treatment process, which indicates the role of WWTPs in the transformation of silver NMs [27]. NMs in biosolids are often land applied such that terrestrial organisms are exposed. NMs that are not removed pass through the WWTPs in the water and are discharged into rivers, lakes, and oceans, where aquatic organisms are exposed [23, 28].

The goal of this research is to understand the fate of ENMs among various phases during activated sludge wastewater treatment. The research will focus on the removal of the ENMs when they enter the wastewater treatment plants, the distribution of the ENMs during the wastewater treatment, and the re-entering of the ENMs to the environment. The objectives of this study to achieve this goal are: (1) to quantify the removal efficiency of silver, titanium dioxide, and carbonaceous NMs from simulated wastewater and into biosolids using lab-scale sequencing batch reactors (SBRs) and (2) to evaluate the effects of NMs on the function of bacteria in WWTPs. By accomplishing these goals, we can develop a

better understanding of the fate of these NMs in WWTPs. Previous studies on NM fate during wastewater treatment have used static batch reactors or predictive life-cycle models [19, 29-31]. Here we operate SBRs for extended periods of time with continuous daily loadings of NMs along with removal of settled effluent and settled biosolids.

Chapter 2

EXPERIMENTAL APPROACH

2.1 SEQUENCING BATCH REACTORS

Laboratory-scale sequencing batch reactors were used in the experiments. For most experiments the reactors had a liquid volume of 1.6 L (Figures A-1A and B provides details); only for a long-term test (150 days) was a slightly different configuration used (Figure A-1C). The long-term experiments were conducted to vary nC_{60} feed concentrations and biomass levels within a continuously operated system. Samples were aerated and mechanically mixed. The reactors were seeded with bacteria culture (return activated sludge) from Northwest Wastewater Treatment Plant in Mesa, Arizona which operated with a sludge retention time close to six days. The reactors were supplied with a previously published synthetic feed solution [32] (detailed composition provided in SI) comprised of salts, trace nutrients, buffer and monosodium glutamate ($C_5H_8NO_4Na$) as a carbon and nitrogen source. This feed solution had a conductivity of 0.5 mS, COD of 780 mg/L, and total dissolved nitrogen (TDN) of 150 mg N/L. Detailed operation and sampling procedures are presented in the Supplementary Information (SI) in Appendix A. Briefly, the hydraulic residence time (HRT) of the SBRs was 8 hours (aeration time) plus settling. The sludge retention time (SRT) was managed in most test at 6.4 days, which is typical for activated sludge systems for COD removal; only in lower TSS tests for the 150-day fullerene tests was the SRT decreased to 4.4 days which was necessary to maintain the lower target TSS level. HRT and SRT were regulated by removing settled supernatant and mixed suspended solids.

4

Typical wastewater treatment systems operate at TSS levels of 1500 to 2500 mg/L, and this was the target level for most experiments. Lower TSS levels were targeted during the 150 day SBR experiment to demonstrate in continuous flow operation the effect of biomass levels of nanomaterials removal. Reactors were operated for several weeks to reach steady state, which was determined on the basis of consistent total suspended solids (TSS) concentration and effluent chemical oxygen demand (COD), before addition of NMs began. Control reactors were operated with (1) the feed solution with NMs but no biomass and (2) the feed solution with no NMs.

2.2 PREPARATION OF NANOMATERIAL STOCK SOLUTIONS

Stock suspensions of NMs were prepared using ultrapure water (Milipore Milli-Q) with conductivity < 1.1 µS/cm. Characteristics of the NMs in the stock suspensions are summarized in Table 1 and Figure SI.2. The stock solution of functionalized (carboxyl terminated polymer coating) silver nanoparticles (*fn*-Ag) used the as-received liquid solution (~300 mgAg/L) from the manufacturer (Northern Nanotechnologies, Ontario, Canada). The *fn*-Ag stock solution contained 8% to 10% ionic silver as measured by ion-specific electrode (ISE) (Accumet® Silver/Sulfide, Fisher), which was used in combination with a pH/mV meter (Φ^{TM} 250 series, Beckman) to measure free Ag^+ ions, and confirmed by centrifugal ultrafiltration using a 10 kDa membrane (Amicon). To investigate the potential toxic effects of ionic silver, stock solutions were prepared by dissolving 200 mg Ag from $AgClO_4$ (Sigma-Aldrich) in 1 L of ultrapure water.

5

Titanium dioxide NM stock suspensions were prepared using Hombikat TiO_2 powder (Sachtleben Chemie GmbH, Duisburg, Germany). Hombikat TiO_2 has a low iso-electric point ($pH_{ZPC} \sim 5.3$ as estimated using a ZetaPALS instrument, Brookhaven Instruments, NY). The stock suspension was prepared by suspending 1 g of TiO_2 into 1 L of ultrapure water and sonicating it with an ultrasonic probe (5T Standard Probe, Model 2000U, Ultrasonic Power Cooperation, Freeport, IL, USA) for 2 hours at 200 W/L. Portions of the suspension were centrifuged at 1000 G for 30 min, and the supernatant was used as the stock TiO_2 suspension (n-TiO_2). The stock solution contained 320 mgTi/L. XRD results indicate that all TiO_2 is pure anatase (Figure A.2). Suwannee River natural organic matter (NOM) (International Humic Substances Society) was added during select experiments.

Fullerene (C_{60}) and hydroxylated-fullerene ($C_{60}(OH)_{24-y}Na_y$) were purchased from MER Corporation, Tucson, Arizona. Aqueous fullerene (nC_{60}) was prepared by adding ~500 mg of C_{60} dry powder to 1L nanopure water and sonicating at 200W/L for 6 hours. The solution was then filtered (Whatman GFF) and permeate became the stock solution. The fullerol stock solution was prepared similarly by adding ~70 mg of n-$C_{60}(OH)_{24-y}Na_y$ to 500 mL ultrapure water, sonicating for 30 minutes, and then filtering.

Table 1 – Summary of Engineered nanomaterials properties

| Nanomaterial | Supplier | Dosage applied to SBR (mg/L) | DLS Mean Diameter (nm) | | Zeta Potential at pH 7 (mV) |
			In Nanopure Water (Polydispersity)	In SBR Feed Solution	
fn-Ag	Northern Nanotech (Vive Nano)	0.5 to 1.5	~5 (0.322)	~30	-6
n-TiO$_2$	Hombikat	0.5 to 2.0	~20 (0.233)	~1700	-30
*Aq-n*C$_{60}$	MER Corp	0.5 to 2.5	~88 (0.172)	~129	-52
n-C$_{60}$(OH)$_x$(ONa)$_y$	MER Corp	2.5	~40 (0.128)	~90	-21

2.3 ANALYTICAL METHODS

Organic carbon substrate utilization by the biomass was assessed using COD, which was measured via the closed reflux dichromate colorimetric method 5220 D (Standard Methods for Water and Wastewater Analysis) [33]. Sample pH was also measured (Beckman Φ250 pH/Temp/mV Meter, Beckman Coulter Inc, Fullerton, CA, USA). Dissolved organic carbon (DOC) and total organic carbon (TOC) concentrations were analyzed using a TOC instrument (Shimadzu TOC-V CSH). Biomass concentration was determined as the TSS concentration following the Standard Methods for Water and Wastewater Analysis [33].

Metal concentrations in liquid samples were determined by acid digestion followed by analysis using Inductively Coupled Plasma-Optical Emission Spectroscopy (ICP-OES) (Thermo iCAP6300 ICP-Optical Emission Spectrometer).

Detection limits were below 1 µg/L. Liquid aliquots of silver nanoparticle dispersions were digested in concentrated ultrapure nitric acid with addition of 30% H_2O_2 using a hotplate digestion method [33]. Liquid aliquots of titanium dioxide nanoparticle dispersions were converted to titanium ions by digestion in a mixture of ultrapure concentrated nitric and sulfuric acids at $T > 220^0C$ using a hotplate digestion method [33]. Recovery of metals from nanoparticle was between 90% and 110%, within acceptable USEPA ranges. Metal concentrations in dry biomass samples were determined by filtering (Whatman GF/F filter) and drying the biomass at 105^0C to constant mass prior to acid digestion. Dry biomass was digested following USEPA SW-846, Method 3050B [33].

Concentrations of fullerenes and fullerols were analyzed using a UV/VIS spectrophotometer (HACH DR5000) at 347 nm and 400 nm, respectively, during short-term SBR tests. During long-term SBR tests (150 days) using fullerenes, nC_{60} was measured after liquid-liquid extraction (10 mL sample, 30 mL glacial acetic acid to prevent emulsion formation, 10 mL toluene) followed by LC/MS (days 0 to 45) and then HPLC (days 45 to 150) following established methods [34-36]; comparable results for the two methods obtained between days 30 and 60 validated the switch to the easier HPLC method. Both methods had detection limits of 1 µg/L when the toluene extract was reduced to 0.5 mL prior to analysis.

Scanning electron microscopy/focused ion beam microscopy equipped with an energy dispersive X-ray microanalysis system (SEM/EDS) (FEI Nova 200 SEM/FIB with EDAX) and transmission electron microscopy (TEM) equipped with EDS (Philips CM200 FEG TEM/STEM with EDAX) was used to characterize

the nanoparticles visually and determine their presence in the biomass. Zeta potential and particle sizes were estimated using the phase analysis light scattering technique (PALS) (ZetaPALS Brookhaven Instruments, Brookhaven, NY). PALS particle sizes were estimated using the monomodal size distribution (MSD). X-ray diffraction (Siemens D5000, CuK_α X-ray source) was used to characterize the crystallographic structure of NMs.

Chapter 3

RESULTS AND DISCUSSION

3.1 INFLUENCE OF NANOMATERIALS ON SUBSTRATE UTILIZATION AND BACTERIAL GROWTH

NM dosages of 0.5 to 2.5 mg/L were applied to SBRs, which were operated for several weeks (Table 1). Organic carbon substrate utilization by the bacterial biomass was assessed by analyzing COD in the effluent. Over a 27-day operation period, influent COD levels in the feed solution averaged 748 ± 13 mg/L. The average COD level of the settled effluent from SBRs without NMs was 64 ± 28 mg/L. The average (27-day operation) COD in the settled effluent from SBRs with fn-Ag and n-TiO$_2$ were 45 ± 12 mg/L and 45 ± 16 mg/L, respectively. SBRs supplied with ionic silver (AgClO$_4$) had an average COD in the settled effluent of 39 ± 19 mg/L. Effluent COD from the SBRs with fullerene and fullerol were 21 ± 8 mg/L and 32 ± 12 mg/L, respectively. Plots of COD in SBR settled effluents are presented in Figure 1. Based on an F-test, effluent COD levels in SBRs with and without NMs were not statistically different ($p > 0.07$). Thus in our study, under the TSS levels (see below) and NM dosages reflective of the upper limit of expected environmental concentrations, the presence of NMs did not adversely affect COD removal in the biological reactors.
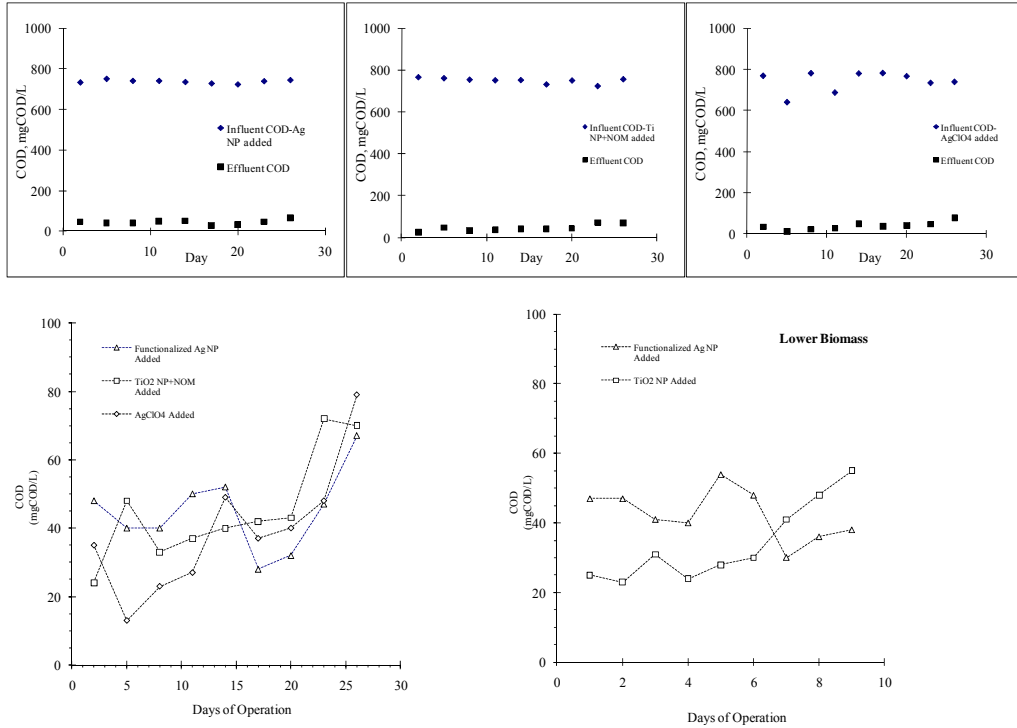
Figure 1 – Plots of COD concentrations over time during operation of the SBRs. The top three plots show influent and effluent COD concentrations for the 27-day SBR tests. The bottom left plot shows only effluent COD concentrations in reactors containing NMs or silver ions. The bottom right plot shows COD removal in NM-containing reactors that were operated only for 9 days.

To further confirm that NMs had minimal impact on COD removal, COD removal kinetics were evaluated during individual loading cycles. For example, in a control SBR without NMs, COD levels rapidly decreased from 804 mg/L to less than 35 mg/L within 2 hours and then remained relatively constant for the duration of the loading cycle (Figure 2). The pseudo first-order rate constant for the loss of COD over the first two hours of the cycle was approximately 1.5 hr^{-1}, and was not

11

different in the presence or absence of NMs. The only exception occurred with an initial addition of fullerol, as approximately 6 hours were required to achieve the effluent COD level on the first day of fullerol addition. This slower COD removal disappeared during subsequent operational cycles. Although the antimicrobial activity of silver nanoparticles and silver ions exists [37, 38], the functional redundancy of the microbial community may have ensured that the biomass removed COD when the systems operated at a TSS value similar to that of a full-scale activated sludge process.
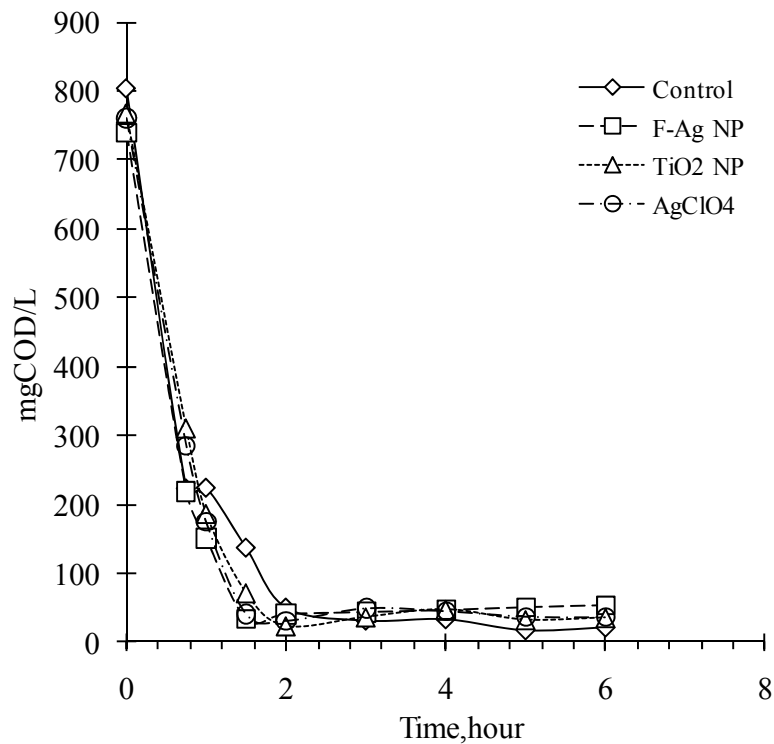

Figure 2 – COD removal kinetics during day 6 of the 4-week SBR testing.

The biomass concentration, measured as TSS, was relatively constant for most SBR experiments (Figure 3). Fullerene and fullerol addition resulted in similar TSS

levels as the controls and exhibited no long-term detrimental influence on COD removal. Biomass concentrations were also constant with n-TiO$_2$ (average 1.3 ± 0.2 gTSS/L). Biomass concentrations were similar to controls for fn-Ag (average 1.8 ± 0.2 gTSS/L) and AgClO$_4$ (average 1.7 ± 0.2 gTSS/L), except during the first operational cycle of feed solutions containing NMs was a significant change (10% to 15% decline) in TSS observed. This could suggest an initial shock from the NMs, or silver ions, after which the mixed microbial community adapted to their presence.
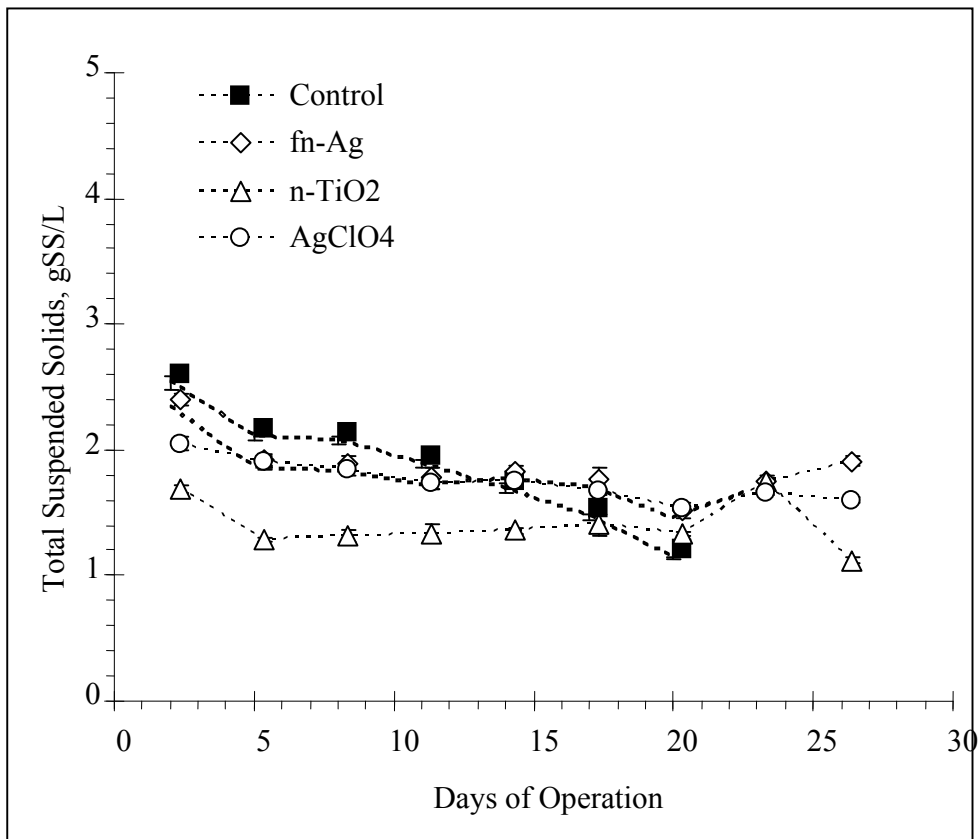
Figure 3 – Biomass concentrations over time in SBRs without NMs (control) or with various NMs added.

3.2 NANOMATERIAL REMOVAL FROM THE LIQUID PHASE IN SEQUENCING BATCH REACTORS

Nanomaterial Removal without Biomass The *fn*-Ag was not removed in absence of biomass (control) experiments (Figure 4), as the influent and settled effluent silver concentrations were comparable. Fullerol was also stable in the feed solution and was not removed during the operation of SBRs without biomass (data not shown). In contrast, in control tests approximately 70% of the nano-scale titanium dioxide (*n*-TiO$_2$) was removed during each SBR loading cycle (Figure 5).

14

Removal of n-TiO$_2$ without biomass present was presumably due to aggregation and sedimentation (abiotic mechanisms) caused by the modest ionic strength present in the feed solution and the time permitted for settling prior to removal of the supernatant at the end of each SBR cycle (i.e., settled effluent). When the n-TiO$_2$ was added into the feed solution, the nanoparticles rapidly aggregated and formed large particles (>1 mm). In an attempt to stabilize n-TiO$_2$ in the control reactors, 5 mgDOC/L of NOM was fed with n-TiO$_2$. However, NOM had minimal effect on n-TiO$_2$ removal, presumably because divalent cations (Mg^{2+} and Ca^{2+}) present in the feed solution still complexed with the NOM coatings on the NMs and facilitated their aggregation [39].
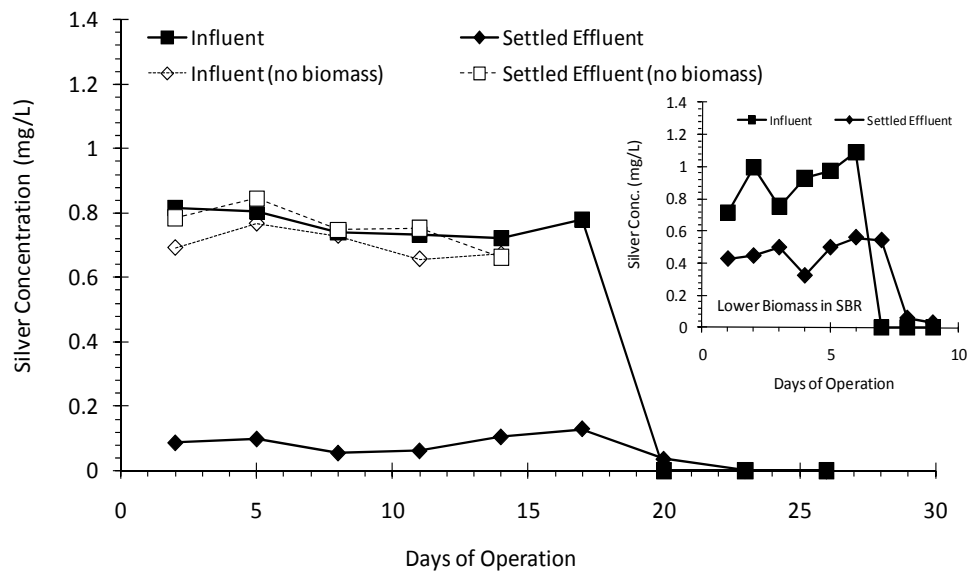
Figure 4 – Silver concentrations in SBRs either without biomass (open symbols) or with biomass (solid symbols; biomass concentration ranged from 2 to 2.5 mgTSS/L). Inset shows lower silver removal results for shorter-term (9-day) experiments (biomass concentration ranged from 1.2 to 1.5 mgTSS/L).

16
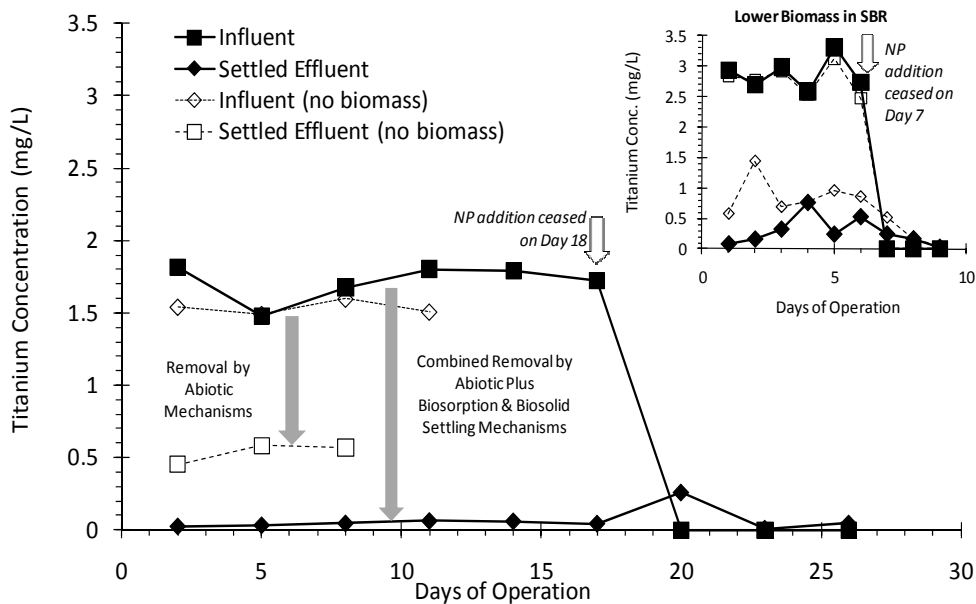
Figure 5 – Titanium concentrations in SBRs either without biomass (control, open symbols) or with biomass (solid symbols; biomass concentration ranged from 1.5 to 2.0 mgTSS/L). Inset shows results for control (no biomass) and short-term (9-day) experiments (solid symbols; biomass concentration ranged from 1.2 to 1.5 mgTSS/L).

Fullerenes were stable in the feed solution during operation of the SBR without biomass for 3 days. After that, the average colloid diameter measured by DLS increased from 129 nm to 632 nm, and the concentration decreased (Figure 6a). We speculated that the cause was bacterial growth in the feed solution even though no biomass was added. Therefore, another SBR was started with feed solution containing fullerenes as well as a biocide (100 mg/L of sodium azide). Fullerenes remained stable in this feed solution (i.e., no removal caused by aggregation and sedimentation) (Figure 6b).
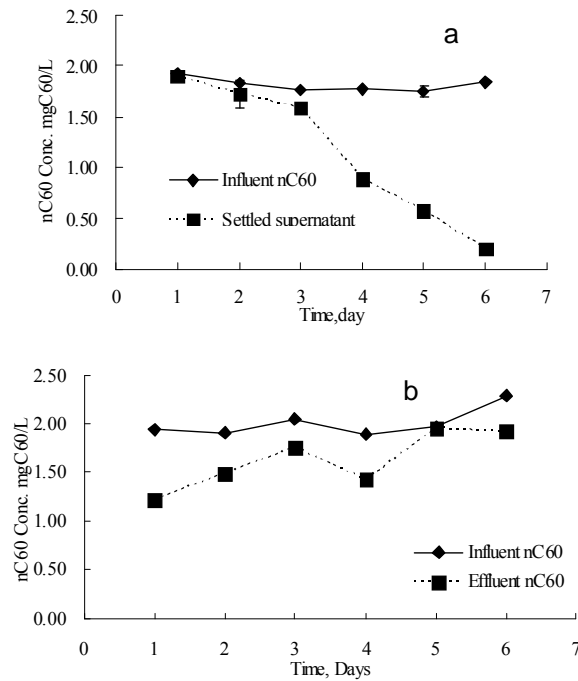
Figure 6-Fullerene (C_{60}) concentrations in an SBR without biomass during a 6-day operation experiment without (a) and with (b) sodium azide.

NM Removal in the Presence of Biomass NMs were loaded continuously during each operational cycle (cycled aeration, withdrawal of mixed suspended solids for SRT management, settling, withdrawal of settled supernatant for HRT management, replenishment with fresh feed solution containing NMs) for a fixed duration to study NM removal, and then the reactors operated with replenishment of the feed solution only (no NMs added) to evaluate "washout" from the reactor. Figure 4 shows influent and effluent silver data for *fn*-Ag in reactors both with and without biomass added. In the presence of biomass (1.8 ± 0.2 mgTSS/L; Figure 3) after reaching steady state, $88\% \pm 4\%$ of the *fn*-Ag was removed from settled supernatant (i.e., effluent) when fresh NMs and feed solution were added during

18

each operational cycle (days 1 through 18). After day 18, replenishment of the feed solution without NMs continued (i.e., zero silver in the SBR influent). Effluent silver concentrations took an additional few days to reach influent levels, which indicates a slow "washout" of silver after ceasing *fn*-Ag addition into the SBR (feed water without NMs was added after day 18). Operation of a 9-day SBR test at a lower biomass concentration (1.1 ± 0.2 mgTSS/L) resulted in 49% ± 10% removal of silver while *fn*-Ag was added (Figure 4 inset). Again, after cessation of *fn*-Ag addition on day 7, a short washout period of silver from the reactor was observed.

Another SBR was then operated for 30 days with an average influent *fn*-Ag concentration of 2.0 ± 0.1 mg/L and a TSS of 0.55 ± 0.10 gSS/L (Figure A.3). The settled supernatant was sampled directly as well as filtered using 0.45-μm membranes and 10 kDa centrifugal ultrafiltration membranes. During this period the silver removal in the settled, 0.45-μm membrane-filtered, and 10 kDa membrane-filtered effluent averaged 58 ± 18%, 88 ± 15%, and 99 ± 0.1%, respectively; the filtered effluent always had a larger removal than the settled effluent. Therefore, a fraction of the silver was associated with colloidal cellular material (i.e., between 0.45-μm and 10kDa) that did not completely settle during the cyclic operation (i.e., it was present in the supernatant). In separate experiments using the stock solution, the 10kDa membranes retained *fn*-Ag and allowed ionic silver to pass through. Thus ionic silver was concluded not to be present in the SBR effluent. Ionic silver could have precipitated as silver chloride or silver sulfide, or adsorbed onto biomass. TEM analysis was conducted on silver nanoparticles in the settled biosolids (Figure SI.8). The size and shape of the silver in the biosolids were

19

consistent with the initial *fn*-Ag nanoparticles, and EDX confirmed them as silver. Therefore, a significant portion, if not all, of the *fn*-Ag nanoparticles did not undergo dissolution and where incorporated into the settled biosolids.

Ionic silver was 8% to 10% of the total silver in the *fn*-Ag stock solution. Therefore, the fate of ionic silver was investigated in a separate SBR operated similarly to that for *fn*-Ag. The biomass concentration over the 27-day experiment averaged 1.8 ± 0.2 mgTSS/L (Figure 3). The average silver removal was $94 \pm 3\%$; the influent ionic silver concentration was 0.90 ± 0.03 mg/L. Ionic silver readily sorbs to wastewater biomass [40]. However, in control experiments (no biomass) with ionic silver, silver was removed from the supernatant, which suggests that precipitation of ionic silver could have occurred. The feed solution contained 0.25 mM chloride. Silver chloride is highly insoluble ($K_{sp} = 1.56 \times 10^{-10}$), and the predicted silver ion concentration in the feed solution at equilibrium would be no more than 0.065 mgAg/L.

Figure 5 shows the influent and effluent titanium concentrations for addition of TiO_2 to SBRs. The removal of titanium increased from 65% in the absence of biomass to $97 \pm 1\%$ with biomass present (1.3 ± 0.2 mgTSS/L). Experiments were not conducted with ionic titanium because of its extremely low solubility.

Initial experiments using fullerols and fullerene were conducted for 6 days of NM loading plus 3 days for washout, and the NM concentrations were quantified by absorption spectroscopy. Fullerol removal determination was based upon absorbance measurements at 400 nm. Influent solutions containing fullerols had an average absorbance of 0.0447 ± 0.0009 cm^{-1}. The settled effluent had an

absorbance of 0.0114 ± 0.0037 cm^{-1}, which equates to roughly 75% fullerol removal. On the basis of an influent fullerene concentration of $\sim$2 mg/L (absorbance at 347 nm of 0.0687 ± 0.0011 cm^{-1}), the settled effluent consistently contained less than 5% of the influent concentration (i.e., >95% removal). Quantification of higher removals was complicated by the presence in the settled effluent of organics that also had absorbance at 347 nm. The day 6 sample underwent solid phase extraction and LC/MS following methods outlined elsewhere [41]; this analysis suggested that very low concentrations of fullerenes were present (<0.1 mg/L, which equates to >95% removal). However, extraction and low-level quantification is more difficult for fullerols than for nC$_{60}$ and was not undertaken here [42].

To document the long-term and variable operation of SBRs, continuous daily nC$_{60}$ loading into a SBR was conducted over nearly 5 months. Biomass concentrations and nC$_{60}$ loadings were intentionally varied (Figure 7). The influent nC$_{60}$ concentration was 0.76 mg/L during Phase 1 (Day 0 to 90). During the first 30 days the biomass concentration was maintained at 1.8 to 2.2 g/L, and the nC$_{60}$ concentration in the settled supernatant averaged 0.03 mg/L (96% removal). The biomass concentration was then gradually decreased to 0.6 g/L by Day 60 by supplying less carbon substrate (COD = 500 mg/L) and reducing the SRT from 6.4 days to 4.4 days. From Day 60 to 90, the nC$_{60}$ concentration in the settled supernatant averaged 0.06 mg/L (92% removal). Despite the 70% decrease in biomass, high removals of nC$_{60}$ persisted. During Phase 2 (Day 90 to 120) the influent nC$_{60}$ concentration was reduced by a factor of 10 to 0.07 mg/L while

maintaining the biomass concentration at 0.6 g/L. The nC$_{60}$ concentration in the settled supernatant averaged 0.002 mg/L (97% removal). During Phase 3 (Day 120 to 150) the influent nC$_{60}$ concentration was increased to 2.0 mg/L while maintaining the same biomass (0.6 g/L). The nC$_{60}$ concentration in the settled supernatant averaged 0.35 mg/L (83% removal). These experiments indicate excellent removal of nC$_{60}$ under typical activated sludge biomass concentrations (>1.5 g/L), although some nC$_{60}$ was always detectable in the settled supernatant (i.e., simulated WWTP effluent). Under very low biomass conditions and very high nC$_{60}$ loadings (e.g., Phase 3), fullerene removal began to deteriorate.
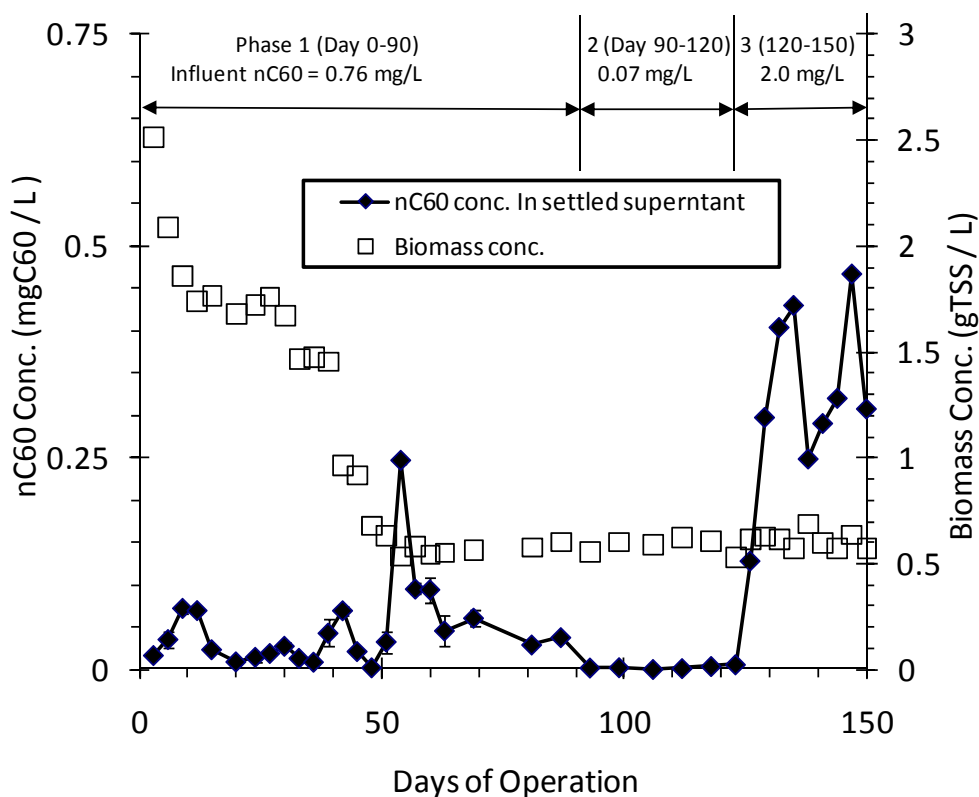
Figure 7 - Variation of nC_{60} concentration in settled supernatant during long-term operation of the SBR. During Phase 1 the influent nC_{60} was maintained at 0.764 mg/L and biomass concentration intentionally decreased. During Phases 2 and 3 the biomass concentration was maintained at a low level and nC_{60} intentionally varied.

3.3 NANOMATERIAL ACCUMULATION IN BIOSOLIDS AND MASS BALANCE

Biosolid samples were collected from the SBRs once per day to manage the SRT. These samples were collected at the end of each complete mixing and aeration period (i.e., mixed liquor), prior to the settling period. The presence of NMs in

biosolids was confirmed by TEM-EDX or SEM-EDX analysis (Figures 8 and 9). Clusters of aggregated n-TiO$_2$ with a size of several hundred nanometers were present in the biosolids. In contrast, individual 1- to 20-nm silver NMs were observed in the biosolids after application of *fn-Ag*. On the basis of TEM analysis, the silver present in the biosolids had a similar size, morphology, and crystalline structure as the *fn-Ag* applied, suggesting that the NMs largely were not transformed but rather sorbed to the biosolids. Most of the silver and titanium dioxide remained in nanoparticle form.
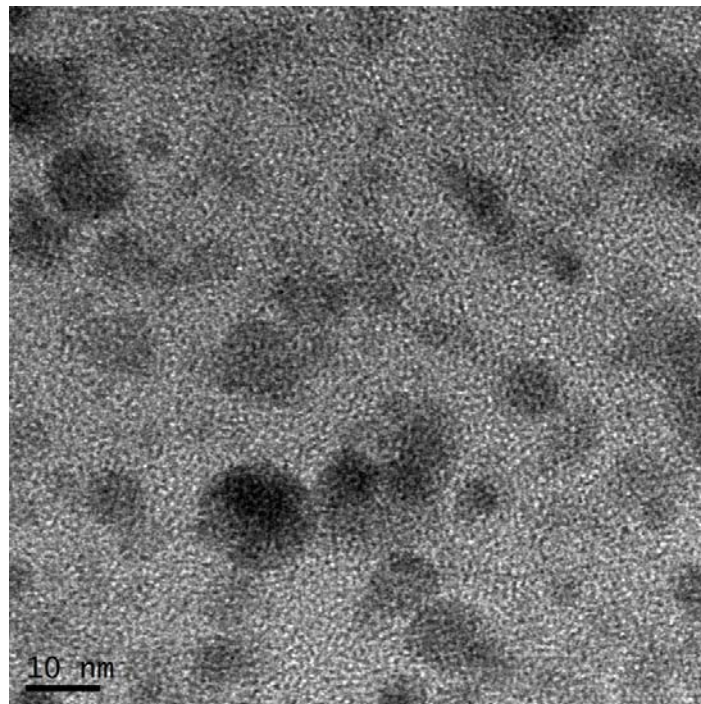

Figure 8 – TEM of biomass sample from the *fn-Ag* SBR. Dark masses are silver (confirmed by EDS). Other TEM images show that these dark masses have crystal structures similar to the initial *fn-Ag* added to the reactors.
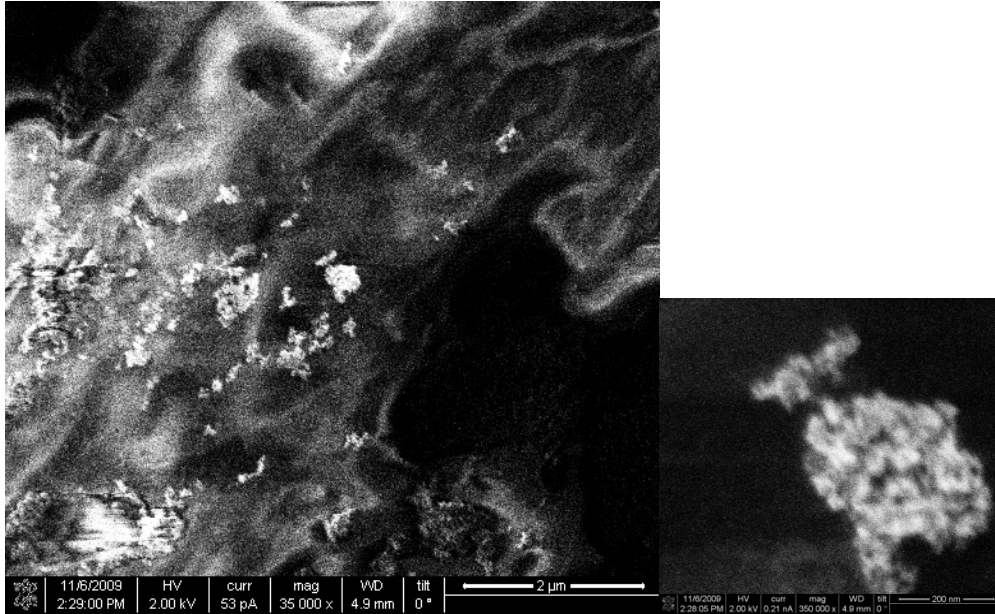
Figure 9 – SEM image (left) of titanium dioxide on biomass shown in backscatter mode (white is the heavier metal titanium). The smaller image (right) shows a close-up of one titanium dioxide aggregate present in the biosolids.

Silver and titanium concentrations in aggregated biosolid samples from the 27-day SBR tests are presented in Figure 10. The data initially showed a gradual increase in the total metal (Ag or Ti) concentration in the biosolids, which began to plateau after 15 to 18 days of SBR operation, approximately three times the SRT value of 6.4 days. After reaching the plateau the biosolids contained approximately 3 mgAg/gSS and 8 mgTi/gSS, respectively; that is, the titanium concentrations were roughly 2.5 times higher than the silver concentrations. This is consistent with the higher removal of titanium (1.7 mgTi/L) compared with silver (0.7 mgAg/L) observed in the SBR (Figures 4 and 5); approximately 2.4 times more titanium than silver was removed.
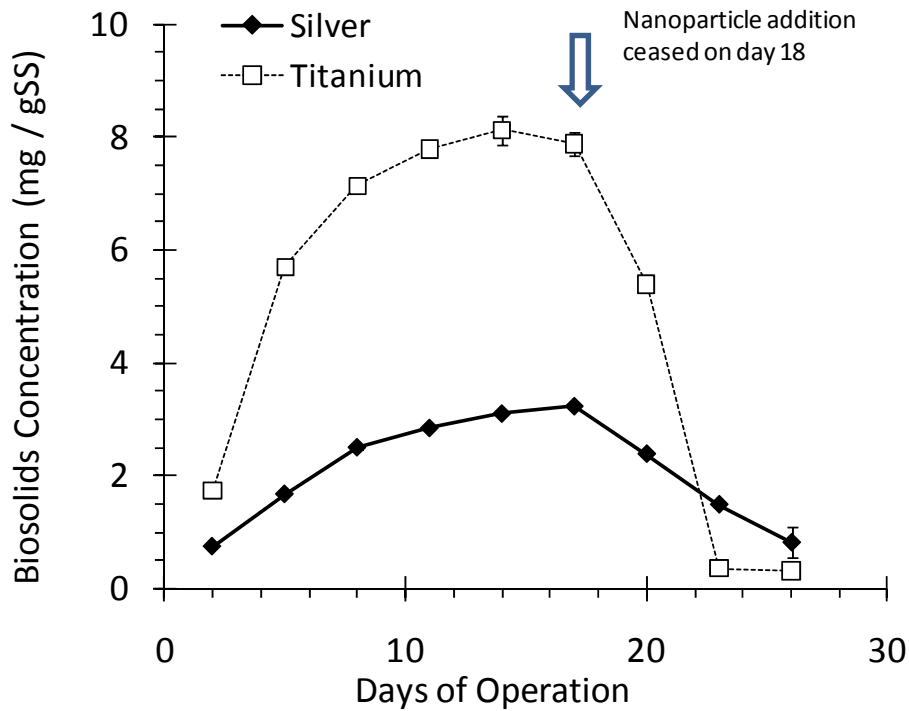
Figure 10 – Change in silver or titanium biosolid concentrations during NM loading (day 0 to 18) and after cessation of NM loading (after day 18) in the SBR.

To demonstrate that the bioreactors would reach a steady-state NM concentration in the biomass, an SBR was operated continuously for 30 days with a fresh *fn*-Ag loading of 2 mgAg/L in each cycle. The silver concentration in the biomass (Figure A.4) reached a plateau at ~9mgAg/mgTSS after 10 days. SBRs must be operated for several SRTs to reach equilibrium because new biomass is growing and because biomass is physically removed from the reactors (to control the SRT). New biomass may adsorb the NMs, thus increasing the concentration of silver in the biosolids, whereas the removal of biomass will decrease it. This increase and decrease may reach equilibrium after a sufficient period of operation.

The two *fn*-Ag experiments with 2 mgAg/L (Figures A.3 and A.4) resulted in roughly 3 times higher silver concentration in the biosolids than the 0.8 mgAg/L (Figures 4 and 10), which shows that higher silver loadings lead to higher steady state biosolids concentrations of silver; the 2 mgAg/L experiment was operated at a slightly lower steady state biomass concentration (0.6 mgTSS/L; Figure A.3) than the 0.8 mgAg/L experiment (1.8 ± 0.2 mgTSS/L; Figure A.3) which accounts for the slightly higher silver concentration in the higher silver loading experiment. Overall, the results implied that short-term operation of SBR reactors (i.e., less than 2 to 3 times the SRT value), or even batch isotherm tests, may not accurately represent the accumulation of NMs in biosolids in a real WWTP.

Combining data for NM concentrations in settled effluent with mixed liquor samples allowed for NM mass balances to be conducted. Over the course of the SBR experiments, mass balances between metal loading and measured metal concentrations were in good agreement (<10% difference). Several mass balance plots are presented in Figure A.5. Closure of the mass balances is important because it confirms that other NM loss mechanisms, such as NM sorption to the reactor or attachment to bubbles (i.e., aerosolization), were negligible in the SBRs.

Chapter 4

CONCLUSION AND FUTURE WORK RECOMMENDATION

Overall, the data collected indicate that biological wastewater treatment plants operated using suspended biomass (e.g., activated sludge) have the potential to remove engineered nanomaterials from wastewaters. Both small, negatively charged NMs (e.g., *fn-Ag*) and larger aggregates of NMs (e.g., *n-TiO₂*) are removed by interaction with biomass in systems operated with TSS similar to that of full-scale WWTPs. The mechanisms of these interactions between NMs and bacteria appear to involve electrostatic attraction and to be size dependent [43, 44]. It is apparent that in our SBRs and other batch experiments that higher biomass (TSS) concentrations improved NM removal [45]. Thus, systems operated with even higher TSS levels than those selected here, which represent common activated sludge systems, could be expected to remove NMs more efficiently. For example, membrane bioreactors (MBRs) often operate with biomass concentrations on the order of 10 gTSS/L. In addition to operating at higher biomass concentrations, the 0.1- to 0.4-μm membrane employed by MBR systems would likely improve overall silver removal compared with sedimentation alone. Many older or smaller WWTPs employ fixed-film biological reactors (e.g., trickling filters) rather than the suspended biomass systems simulated here, which are used by activated sludge systems. Further research into NM removal by attached microbial communities is therefore needed.

As NM removal from wastewater occurs, NMs become concentrated in biosolids. Roughly 6 to 8 million tons of municipal waste biosolids are produced

annually in the USA [46], and this amount is increasing because of the commissioning of new plants and upgrades of existing facilities [47]. Approximately 60% of the biosolids in the USA are applied to land, 22% incinerated, and 17% landfilled [46], but the trends are regionally variable. There is considerable debate about the proper disposal for biosolids [48]. On one hand, land application of biosolids is viewed as a sustainable practice because they provide valuable nutrients and structure to soils. On the other hand, new or more stringent regulations due to a wide array of pollutant could lead to less land application of biosolids and higher rates of incineration [48]. Incineration can recover thermal energy, but it creates new problems associated with particulate emissions and deposition of ashes into landfills. Incineration of biosolids generates particulates containing heavy metals or polyaromatic hydrocarbons [49, 50]. Fly ash is often mixed with biosolids and land applied as a fertilizer [51]. Elements used in NMs (e.g. Ti, Zn) are found in fly ash in concentrations exceeding 3000 ppm [52], but little work has characterized the mineralogy of these residuals. Approximately 170 incinerators treat biosolids within the USA [53] incinerating almost a quarter of biosolids generated in the nation [54]. Incineration is more prevalent in countries with high population density (e.g., the European Union and Japan) where land disposal is not an option or public concern about food chain contamination exists [48, 52, 55, 56]. Additional research is needed to understand the long-term fate of NMs as biosolids are subsequently disposed.

REFERENCES

1.   NNI, N.N.I., *What is nanotechnology?*, 2006: Wilmington, DE: Dupont, and Washington, DC: Environmental Defense.

2.   Maynard, A.D., et al., *Safe handling of nanotechnology.* Nature, 2006. **444**(7117): p. 267-269.

3.   WoodrowWilson. *The Project on Emerging Technologies (http://www.nanotechproject.org/).* 2009.

4.   Thayer, A.M., *Firms find a new field of dreams.* Chem. Eng. News, 2000. **78**(42): p. 36-38.

5.   Muhling, M., et al., *An investigation into the effects of silver nanoparticles on antibiotic resistance of naturally occurring bacteria in an estuarine sediment.* Marine Environmental Research, 2009. **68**(5): p. 278-283.

6.   Ramsden, C.S., et al., *Dietary exposure to titanium dioxide nanoparticles in rainbow trout, (Oncorhynchus mykiss): no effect on growth, but subtle biochemical disturbances in the brain.* Ecotoxicology, 2009. **18**(7): p. 939-951.

7.   Handy, R.D., A.N. Jha, and A. Al-Jubory, *In vitro techniques and their application to nanoparticles.* Comparative Biochemistry and Physiology a-Molecular & Integrative Physiology, 2009. **153A**(2): p. S87-S87.

8.   Oberdorster, G., V. Stone, and K. Donaldson, *Toxicology of nanoparticles: A historical perspective.* Nanotoxicology, 2007. **1**(1): p. 2-25.

9.   Klaine, S.J., et al., *Nanomaterials in the environment: Behavior, fate, bioavailability, and effects.* Environmental Toxicology and Chemistry, 2008. **27**(9): p. 1825-1851.

10.   Handy, R.D., R. Owen, and E. Valsami-Jones, *The ecotoxicology of nanoparticles and nanomaterials: current status, knowledge gaps, challenges, and future needs.* Ecotoxicology, 2008. **17**(5): p. 315-325.

11. Duran, N., et al., *Antibacterial effect of silver nanoparticles produced by fungal process on textile fabrics and their effluent treatment.* Journal of Biomedical Nanotechnology, 2007. **3**(2): p. 203-208.

12. Tong, Z.H., et al., *Impact of fullerene (C-60) on a soil microbial community.* Environmental Science & Technology, 2007. **41**(8): p. 2985-2991.

13. Cheng, J.P., E. Flahaut, and S.H. Cheng, *Effect of carbon nanotubes on developing zebrafish (Danio rerio) embryos.* Environmental Toxicology and Chemistry, 2007. **26**(4): p. 708-716.

14. Moore, M.N., *Do nanoparticles present ecotoxicological risks for the health of the aquatic environment?* Environment International, 2006. **32**(8): p. 967-976.

15. Oberdorster, E., et al., *Ecotoxicology of carbon-based engineered nanoparticles: Effects of fullerene (C-60) on aquatic organisms.* Carbon, 2006. **44**(6): p. 1112-1120.

16. Robichaud, C.O., et al., *Estimates of Upper Bounds and Trends in Nano-TiO2 Production As a Basis for Exposure Assessment* Environ. Sci. Technol., ASAP.

17. Wiesner, M.R., et al., *Decreasing Uncertainties in Assessing Environmental Exposure, Risk, and Ecological Implications of Nanomaterials.* Environmental Science & Technology, 2009. **43**(17): p. 6458-6462.

18. Nowack, B., *Is anything out there? What life cycle perspectives of nano-products can tell us about nanoparticles in the environment.* Nano Today, 2009. **4**(1): p. 11-12.

19. Gottschalk, F., et al., *Modeled Environmental Concentrations of Engineered Nanomaterials (TiO2, ZnO, Ag, CNT, Fullerenes) for Different Regions.* Environmental Science & Technology, 2009. **43**(24): p. 9216-9222.

20. Mueller, N.C. and B. Nowack, *Exposure modeling of engineered nanoparticles in the environment.* Environmental Science & Technology, 2008. **42**(12): p. 4447-4453.

21. Nowack, B. and T.D. Bucheli, *Occurrence, behavior and effects of nanoparticles in the environment* Environmental Pollution, 2007. **150**(1): p. 5-22.

22. Nowack, B., *The behavior and effects of nanoparticles in the environment.* Environmental Pollution, 2009. **157**(4): p. 1063-1064.

23. Brar, S.K.V., M.; Tyagi, R.D.; Surampalli, R.Y. , *Engineered nanoparticles in wastewater and wastewater sludge – Evidence and impacts.* Waste Management, 2010. **30**: p. 504-520.

24. Kiser, M.A., et al., *Titanium Nanomaterial Removal and Release from Wastewater Treatment Plants.* Environ. Sci. Tech., 2009.

25. Benn, T., *The Release of Engineered Nanomaterials from Commercial Products*, in *School of Sustainable Engineering and The Built Environment*2009, Arizona State University: Tempe, AZ.

26. Limbach, L.K., et al., *Removal of oxide nanoparticles in a model wastewater treatment plant: Influence of agglomeration and surfactants on clearing efficiency.* Environmental Science & Technology, 2008. **42**(15): p. 5828-5833.

27. Kim, B., Park, C.S., Murayama, M., Hochella, M.F., *Discovery and Characterization of Silver Sulfide Nanoparticles in Final Sewage Sludge Products.* Environ. Sci. & Technol., 2010. **44**(19): p. 7509-7514.

28. Nowack, B. and T.D. Bucheli, *Occurrence, behavior and effects of nanoparticles in the environment*, in *Environmental Pollution*2007. p. 5-22.

29. Yin, Y.X., et al., *Examination of purified single-walled carbon nanotubes on activated sludge process using batch reactors.* Journal of Environmental Science and Health Part a-Toxic/Hazardous Substances & Environmental Engineering, 2009. **44**(7): p. 661-665.

30. Jarvie, H.P., Al-Obaidi, H., King, S.M., Bowes, M.J., Lawrence, M.J., Drake, A.F., Green, M.A., Dobson, P.J., *Fate of Silica Nanoparticles in Simulated Primary Wastewater Treatment.* Environ. Sci. & Technol., 2009. **43**(22): p. 8622-8628.

31. Limbach, L.K., et al., *Removal of oxide nanoparticles in a model wastewater treatment plant: Influence of agglomeration and surfactants on clearing efficiency*, in *Environmental Science & Technology*2008. p. 5828-5833.

32. Moussa, M.S., et al., *Modelling nitrification, heterotrophic growth and predation in activated sludge.* Water Research, 2005. **39**(20): p. 5080-5098.

33. APHA, AWWA, and WEF, *Standard Methods for the Examination of Water And Wastewater (21st Edition)*2005, Washington, DC: American Public Health Association.

34. Benn, T., P. Westerhoff, and P. Herckes, *Detection of Fullerenes (C60 and C70) in Commercial Cosmetics.* Environmental Engineering Science, 2010. **39** (6): p. 1875-1882.

35. Pycke, B.F., et al., *Strategies for quantifying C60 fullerenes in biological samples and implications for toxicological Studies.* Trends in Analytical Chemistry, 2011. **30**(1): p. 44-57.

36. Benn, T., et al., *Evaluation of extraction methods for quantification of aqueous fullerenes in urine.* Analytical and Bioanalytical Chemistry, in-press.

37. Duran, N., et al., *Antibacterial effect of silver nanoparticles produced by fungal process on textile fabrics and their effluent treatment*, in *Journal of Biomedical Nanotechnology*2007. p. 203-208.

38. Choi, O.K., Hu, Z.Q., *Nitrification inhibition by silver nanoparticles.* Water Sci. & Technol., 2009. **59**(9): p. 1669-1702.

39. Zhang, Y., et al., *Impact of Natural Organic Matter and Divalent Cations on the Stability of Aqueous Nanoparticles.* Water Research, 2009. **43**(17): p. 4249-4257.

40. Adams, N.W.H. and J.R. Kramer, *Silver speciation in wastewater effluent, surface waters, and pore waters.* Environmental Toxicology and Chemistry, 1999. **18**(12): p. 2667-2673.

41.   Chen, Z., P. Westerhoff, and P. Herckes, *Quantification of C-60 fullerene concentrations in water.* Environmental Toxicology and Chemistry, 2008. **27**(9): p. 1852-1859.

42.   Chao, T.-C., et al., *Characterization and LC-MS/MS based quantification of hydroxylated fullerenes.* Analytical Chemistry, in-press.

43.   Zhang, W., A.G. Stack, and Y.S. Chen, *Interaction force measurement between E. coli cells and nanoparticles immobilized surfaces by using AFM.* Colloids and Surfaces B-Biointerfaces, 2011. **82**(2): p. 316-324.

44.   Zhang, W., et al., *Adsorption of hematite nanoparticles onto Caco-2 cells and the cellular impairments: effect of particle size.* Nanotechnology, 2011. **21**(35).

45.   Kiser, M.A., et al., *Titanium Nanomaterial Removal and Release from Wastewater Treatment Plants*, in *Environmental Science & Technology*2009. p. 6757-6763.

46.   Peccia, J. and T. Paez-Rubio, *QUANTIFICATION OF AIRBORNE BIOLOGICAL CONTAMINANTS ASSOCIATED WITH LAND APPLIED BIOSOLIDS*, in *Final Report*2006, Water Environment Research Foundation. p. 169.

47.   NRC, *BIOSOLIDS APPLIED TO LAND: ADVANCING STANDARDS AND PRACTICES*, N.R.C. (NRC), Editor 2002, National Academy Press: Washington, DC. p. 284.

48.   Wang, H.L., et al., *Technological options for the management of biosolids.* Environmental Science and Pollution Research, 2008. **15**(4): p. 308-317.

49.   Shao, J.G., et al., *Emission characteristics of heavy metals and organic pollutants from the combustion of sewage sludge in a fluidized bed combustor.* Energy & Fuels, 2008. **22**(4): p. 2278-2283.

50.   de Velden, A.V., et al., *The distribution of heavy metals during fluidized bed combustion of sludge (FBSC).* Journal of Hazardous Materials, 2008. **151**(1): p. 96-102.

51.   Reijnders, L., *Disposal, uses and treatments of combustion ashes: a review.* Resources Conservation and Recycling, 2005. **43**(3): p. 313-336.

52.   Marani, D., et al., *Behaviour of Cd, Cr, Mn, Ni, Pb, and Zn in sewage sludge incineration by fluidised bed furnace.* Waste Management, 2003. **23**(2): p. 117-124.

53.   EPA, U., *AP 42: Compilation of Air Pollutant Emission Factors, Volume 1: Stationary Point and Area Sources (5th Edition)*, Retrieved from http://www.epa.gov/ttnchie1/ap42/ on January 16, Editor 2009.

54.   USEPA, *Biosolids Generation, Use, and Disposal in the United States*, 1999: Washington DC.

55.   Commision, E., *Pollutants in urban wastewater and sewage sludge. Final Report*, 2001, Office for Official Publications of the European Communities: Luxembourg.

56.   Hara, K. and T. Mino, *Environmental assessment of sewage sludge recycling options and treatment processes in Tokyo.* Waste Management, 2008. **28**(12): p. 2645-2652.

57.   Moussa, M.S., et al., *Modelling nitrification, heterotrophic growth and predation in activated sludge*, in *Water Research*2005. p. 5080-5098.
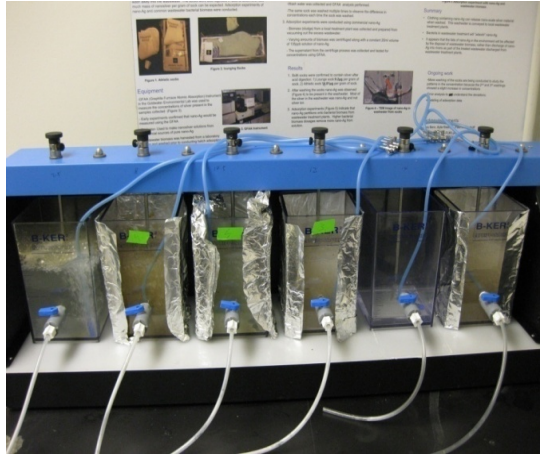
APPENDIX A

SUPPLEMENTARY INFORMATION

Figure A-1A- Photograph of SBRs on a mixing system with aeration tubes (blue).
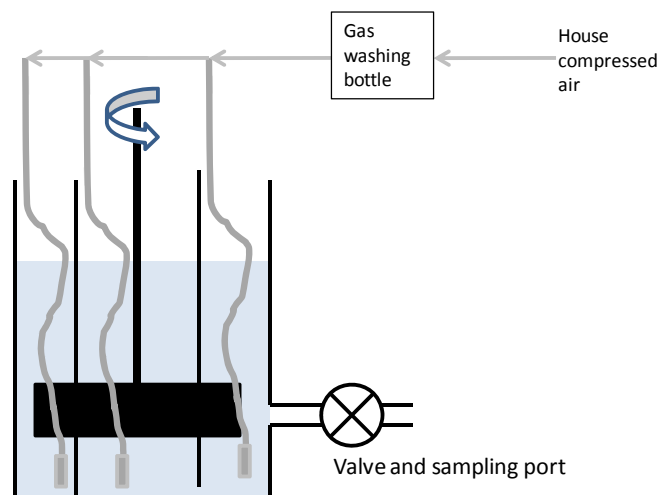

Figure A-1B- Schematic diagram for the SBRs which includes mechanical mixing

provided using a standard apparatus using rotational shafts with rectangular

paddles (1-inch x 3-inch) attached at the end (Stirrer Model 7790-400, Phipps and

Bird, VA) at 120 rpm. Multiple gas diffusion stones (3/8" * 19/16") were used

during aeration and did not interfere with mechanical mixing. The total volume of

the reactor (B-Ker from Phipps and Bird) is 2 L and has dimensions of 7-15/16" H x

4-15/16" W.

Figure A-1C- Reactor (1 gallon glass bottle wrapped in tin-foil) used only for the long-term experiments with fullerenes. 2.5L of solution was contained in the bottle. The HRT was managed by removing 2L of water daily and replacing with fresh feed solution containing NPs. The SRT was managed at 6.4 days for higher TSS tests and 4.4 days for lower TSS tests. Mechanical mixing was provided with a large magnetic stir-bar and mixing sufficient to keep biomass suspended. Aeration was provided using gas diffusion stones (1/2" * 1").

Feed and Trace Mineral Solution Composition

An influent feed solution was prepared to feed the bacteria in the SBRs following a published formulation [57], by dissolving the following ingredients into 1 L of ultrapure water (Milipore Milli-Q) with conductivity < 1.1 µS/cm: (1) 1.002 g of monosodium glutamate ($C_5H_8NO_4Na$) as a carbon and nitrogen source,

(2) 219 mg of potassium dihydrogen phosphate KH_2PO_4 as a phosphorous source, (3) 90 mg of magnesium sulfate heptahydrate ($MgSO_4 \cdot 7H_2O$), (4) 14 mg of calcium chloride monohydrate ($CaCl_2 \cdot H_2O$), (5) 36 mg of potassium chloride (KCl), and (6) 0.3 mL of trace minerals solution (see SI) to enhance bacterial growth. The synthetic feed solution had a conductivity of 0.5 mS, COD of 780 mg/L, and total dissolved nitrogen (TDN) of 150 mg N/L.

The trace minerals solution was prepared by dissolving the following salts in 1 L of ultrapure water: (1) 1.5 g of ferric chloride hexahydrate ($FeCl_3 \cdot 6H_2O$), (2) 0.15 g of boric acid (H_3BO_3), (3) 0.03 g of copper sulfate pentahydrate ($CuSO_4$)$\cdot 5H_2O$, (4) 0.18 g of potassium iodide (KI), (5) 0.12 g of manganese chloride tetrahydrate ($MnCl_2 \cdot 4H_2O$), (6) 0.06 g of sodium molybdenate dihydrate ($Na_2MoO_4 \cdot 2H_2O$), (7) 0.12 g of zinc sulfate heptahydrate ($ZnSO_4 \cdot 7H_2O$), (8) 0.15 g of cobalt chloride hexahydrate ($CoCl_2 \cdot 6H_2O$), and (9) 10 g of Sodium-EDTA [57].

SBR operation and sampling procedure

The reactors were operated in a 10 hr cycle mode that consisted of 8 hours of aeration (using diffusion stones and mechanical mixing), 90 minutes of sludge settling, and 30 minutes of effluent replacement. Before the sludge settling step, 125 mL of the mixed liquor suspended solid was removed and stored for analysis at 4 oC. The effluent replacement included discharge of 875 mL of settled supernatant and addition of 1 L fresh synthetic feed solution. This mode of operation allowed for a Sludge Retention Time (SRT) of 6.4 days.

For the 27-day operated reactor, aliquots (each 25 mL) were collected over six cycle periods (3 days) and combined to obtain 3-day composite influent samples. The 125 mL aliquots obtained from the mixed liquor over six cycle periods were also to form 3-day composite mixed liquor samples. Using the same protocols, 3-day composite effluent samples were also prepared. Additional 20-mL aliquots were sampled over a six cycle periods from the bottom 0.6 L of the control reactors with no biomass, and the samples were combined for a 3-day composite sample. All samples were stored in the dark at 40C before processing and analysis.

For the 150-day fullerene experiment the SRT was maintained at either 6.4 days or 4.4 days, with the later required to achieve steady-state concentrations of lower TSS levels which were desired.   The same HRT was maintained.
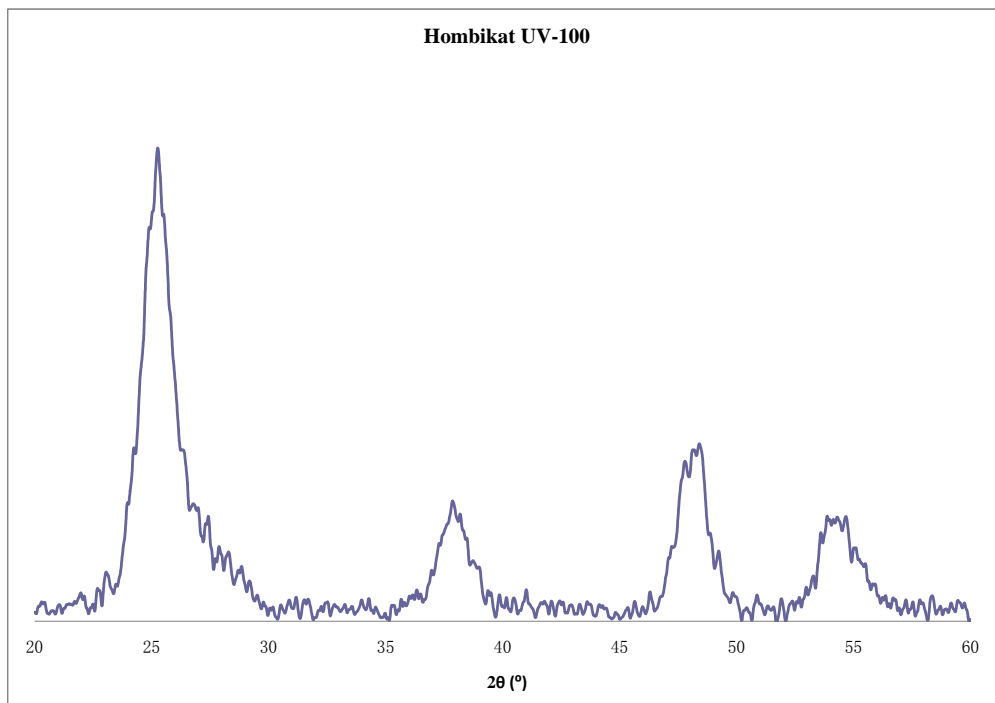

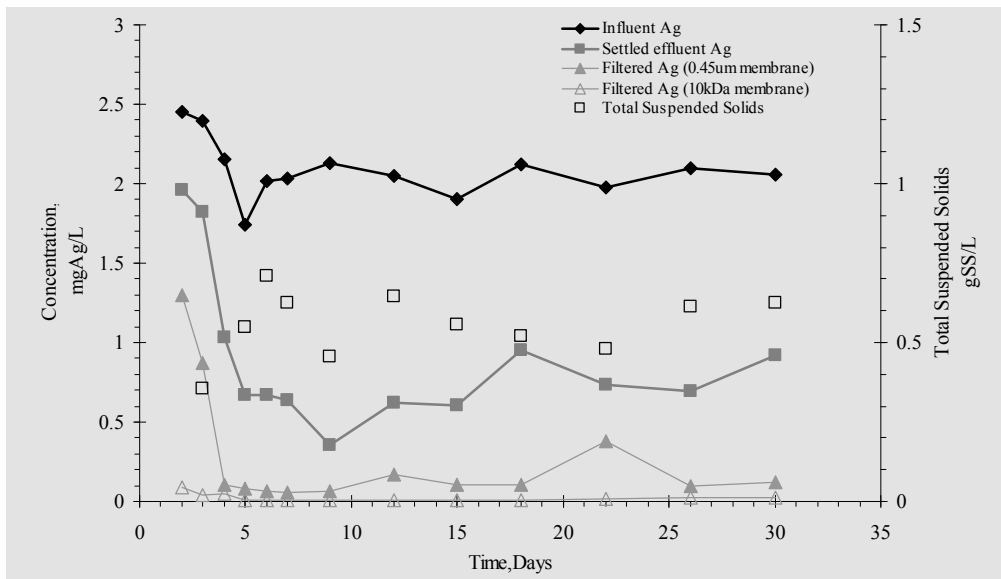Figure A-2 - XRD of HOMBIKAT titanium dioxide nanoparticles.

Figure A-3 - Silver concentrations in the influent, settled effluent, filtered effluent (0.45 μm membrane and 10 kDa membrane) and the total suspended solids in a SBR operated for 30 days.
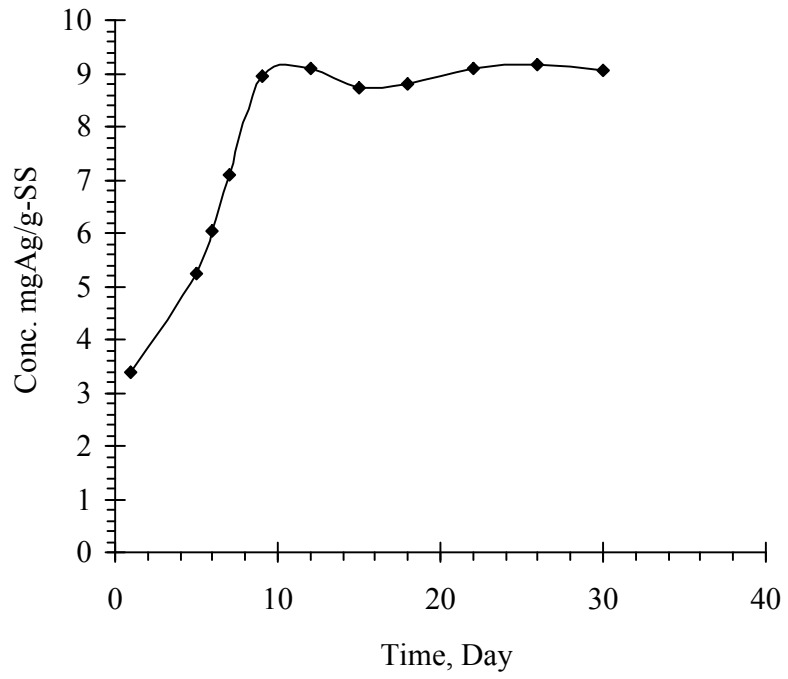
Figure A-4 - Silver concentrations in biosolids from SBRs operated for 30 days
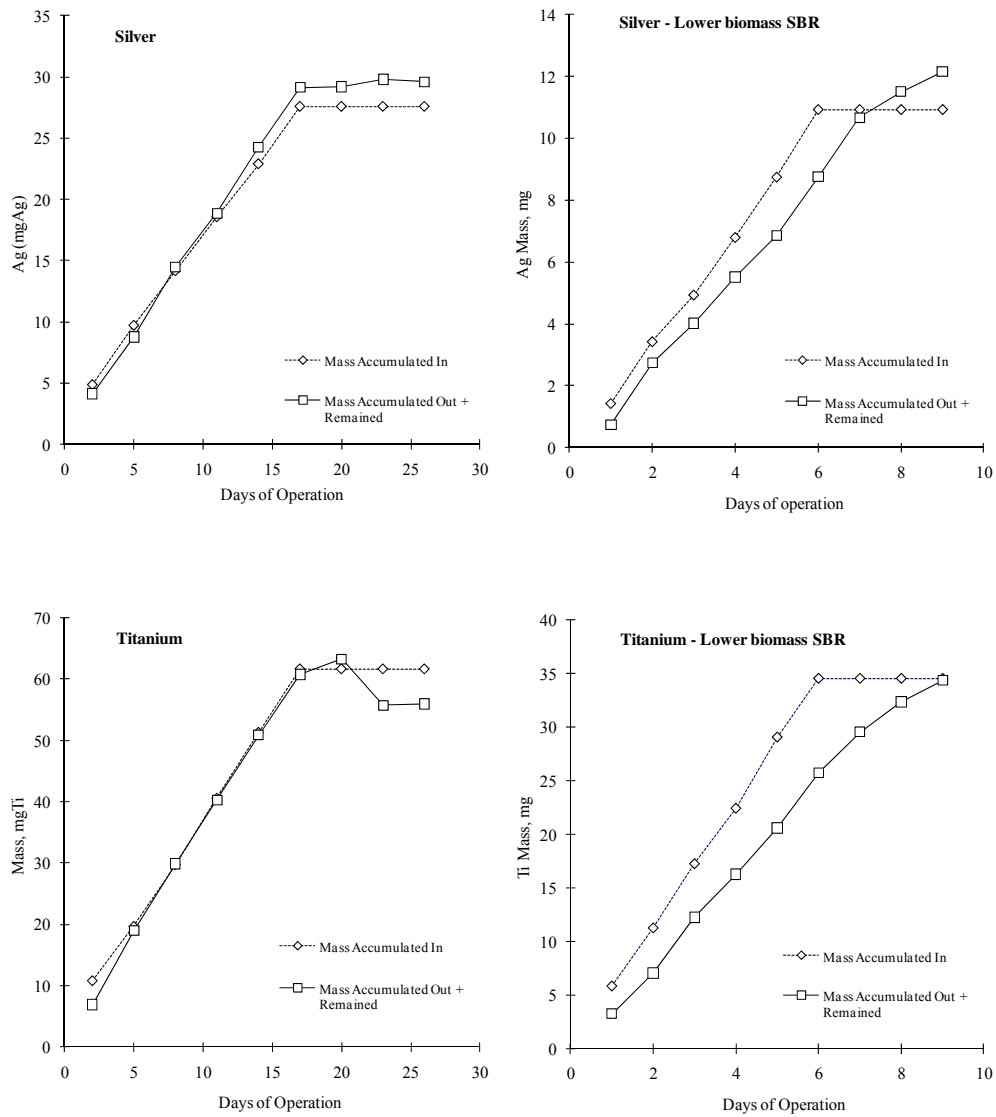
(Figure A.3)

Figure A-5 - Representative mass balances for silver and titanium from SBR tests.